

Electrochemical performance of Ni/TiO₂ hollow sphere in proton exchange membrane water electrolyzers system

Jayeeta Chattopadhyay[†], Rohit Srivastava, and Prem Kumar Srivastava

Department of Applied Chemistry, Birla Institute of Technology, Deoghar Extension Campus,
Jasidih - 814 142, Jharkhand, India

(Received 6 March 2013 • accepted 14 May 2013)

Abstract—This work presents the electrocatalytic evaluation of Ni/TiO₂ hollow sphere materials in PEM water electrolysis cell. All the electrocatalysts have shown remarkably enhanced electrocatalytic properties in comparison with their performance in aqueous electrolysis cell. According to cyclic voltammetric results, 0.36 A cm⁻² peak current density has been exhibited in hydrogen evolution reaction (HER) from 30 wt% Ni/TiO₂ electrocatalyst. 15 wt% Ni-doped titania sample has shown the best result in oxygen evolution reaction (OER) with the anodic peak current density of 0.3 A cm⁻². In the anodic polarization curves, the performance of 15 wt% Ni/TiO₂ hollow sphere electrocatalyst was evaluated up to 140 mA cm⁻² at comparatively lower over-potential value. 20 wt% Ni/TiO₂ hollow sphere electrocatalyst has also shown electrochemical stability in PEM water electrolyzer for 48 h long analysis. The comparative electrocatalytic behavior of hollow spherical materials with non-sphericals is also presented, which clearly shows the influence of hollow spherical structure in greater electrocatalytic activity of the materials. The physical characterization of all the hollow spherical materials is presented in this work, which has confirmed their better electrochemical behavior in PEM water electrolyzer.

Key words: Titania Hollow Sphere, PEM Water Electrolyzer, Electrocatalysts, Nickel

INTRODUCTION

The requirement of a new energy carrier is established and current scenario of hydrocarbon usage as a primary energy source is definitely not sustainable [1]. Hydrogen is the best option as sustainable fuel, and it is considered as one of the potential solutions in the present energy and environmental problems on earth [2]. Proton exchange membrane water electrolyzers (PEMWE) can be used to produce hydrogen from water without forming carbon products. The performance of the PEMWE system mainly depends on the structure and electrochemical characteristics of the electrode materials involved in hydrogen and oxygen evolution reaction. The efficiency of MEA is entirely dependent on the material characteristics of both the electrodes and membranes as well as on the structure of triple-phase boundary [3,4].

It is well-known that the slowest step in water electrolysis is the oxygen evolution reaction (OER). The main energy loss happens during OER in the PEMWE system, as the reaction process is very complicated. This step includes the adsorbed species on the catalyst surface, resulting in the blockage of active sites of the surface, during their oxidation. Thus, efficient electrocatalyst development for PEMWE becomes a technological challenge for its commercialization [2]. Noble metal oxides are well established and popular as electrocatalysts in various industrial electrochemical processes in the form of dimensionally stable anodes (DSA), which is developed by Beer [5]. Several studies have been reported on electrocat-

alytic properties of IrO₂ and RuO₂ in oxygen evolution [6-8]. The application of mixed metal oxides has become popular due to the synergistic effect of individual metal oxides, which have shown improved kinetics of OER. But due to their high price and limited availability, the application of these metals will be limited in the future. Thus, the tendency in the development of modern electrocatalysts is to reduce or completely replace the noble metals. Titanium dioxide is one of the attractive choices as electrocatalysts, due to its low cost, high dielectric constant, purity and homogeneity.

Hollow spherical titania has become highly popular due to its low density, large surface area and void space with tunable shell thickness, so that it can be utilized in catalysis, biomedicine and ferrofluid technology [9,10]. Appropriate loading of a metal on titania hollow sphere can enhance its electrocatalytic activity by a strong metal support interaction (SMSI) effect [11]. Our research group earlier reported the electrocatalytic enhancement of titania hollow sphere with tin [12] and barium [13] loading in water electrolysis. In our recent work, we have reported the enhanced electrocatalytic activity of Ni-doped titania hollow sphere during water electrolysis in acidic media to produce hydrogen and oxygen gases [14]. In that study, we loaded the electrocatalyst ink onto water-proofed carbon cloth and performed various electrochemical characterizations. In the cyclic voltammetric study, the hydrogen evolution peak was quite intense for 30 wt% Ni-loaded TiO₂ hollow sphere electrocatalyst with cathodic peak current density of 32 mA cm⁻². Similarly, oxygen evolution peak in the anodic region was also around 13 mA cm⁻². In the present study, we have examined the Ni-doped titania hollow sphere electrocatalysts in PEM water electrolysis cell, by considering their great electrocatalytic performance during water

[†]To whom correspondence should be addressed.
E-mail: jayeeta08@gmail.com

electrolysis in acidic media.

MATERIALS AND METHODS

1. Hollow Sphere Preparation and Physical Characterizations

Titania hollow spheres were prepared by using soft templating method [15-17], in which poly(styrene-methacrylic acid) latex particles were used as template core material, and then coated with the titania all over the surface. In the final stage, the core material is removed by calcinations at 400 °C. The detailed synthetic process has already been mentioned in the previous work [14]. After the titania hollow sphere synthesis, 15, 25 and 30 wt% of nickel was loaded over spherical structure, as reported earlier. To compare the electrocatalytic behavior of hollow spherical materials with non-spherical nickel-doped titania, co-precipitation method has been utilized. 15 wt% Ni/TiO₂ was synthesized and finally calcined at 400 °C. The surface morphologies of the hollow sphere materials have been characterized with scanning electron microscope (SEM) and transmission electron microscope (TEM) with JSM-6400 and JEM-2010, respectively. The X-ray diffraction patterns were measured by a D/MAX-3C equipment of Rigaku Denki Co. Ltd. by using Cu K α radiation with fixed powder source (30 kV, 15 mA) with the applied scan rate of 2° (2 θ)/min. Specific surface areas of the catalysts were evaluated by Brunauer-Emmett-Teller (BET) surface area analysis with Micromeritics ASAP equipment, model 2010 using N₂ adsorption-desorption isotherms at 77.35 K. The thermal nature of the materials have been executed by thermogravimetric analysis (TGA) with Shimadzu TGA-50H apparatus, by heating the samples up to 725 °C with the 10 °C/min heating rate.

2. MEA Preparations and Water Electrolysis

The spraying technique is taken into account due to its simplicity and easy control of the catalyst loading. In the catalyst ink preparation, catalyst powder was mixed with Nafion® solution (Aldrich, USA) and solvent mixture of water and i-propyl alcohol under sonication bath for 20 mins. The catalyst ink was then casted onto Nafion-115 membrane using spray gun with an approximate catalyst loading of 2 mg cm⁻². Before catalyst loading, Nafion membrane was pretreated with the procedure mentioned by Srinivasan et al. [18].

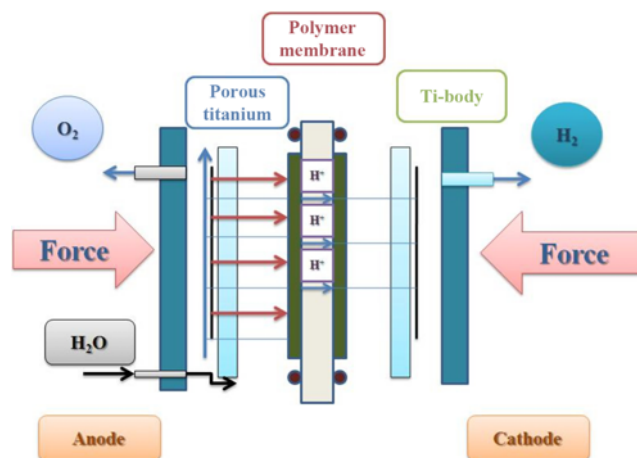


Fig. 1. Schematic diagram of PEM water electrolysis cell.

In the PEM cell, the cathode was prepared by spraying Pt on Vulcan XC-72 R (E-TEK) onto the opposite side of the membrane using similar method as prescribed in the anode. The Pt loading was 0.5 mg cm⁻² in the cathode. After spraying, the MEA was hot pressed at 110 °C and 15 kg cm⁻² for 5 min, followed by boiling in dil. HCl and deionized water repeatedly. Porous titanium sinters were then pressed against these catalytic layers to provide the electrical contact. Ag/AgCl in 3 M KCl solution is used as reference electrode and Pt plate as counter electrode in 0.1 N H₂SO₄ solution. The electrode arrangement is shown in Fig. 1. All electrochemical measurements were performed in a Potentiostat/Galvanostat (Princeton Applied Research, Parastat® 4000).

RESULTS AND DISCUSSION

SEM images of pure TiO₂ and 30 wt% Ni/TiO₂ hollow spheres are shown in Fig. 2(a) and (b). The micrographs have confirmed the spherical structure of the materials with morphological changes on the surface with nickel loading. The surface of the pure TiO₂ sample is smoother than the nickel loaded one. Fig. 3 presents the TEM image of 30 wt% nickel doped titania hollow spheres. The

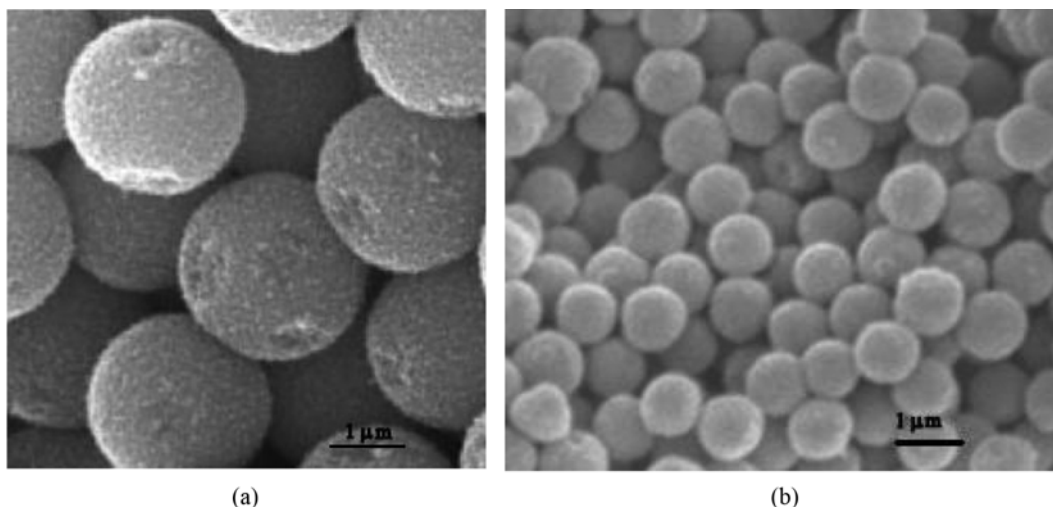


Fig. 2. (a) and (b): SEM images of pure TiO₂ and 30 wt% Ni/TiO₂ hollow spheres.

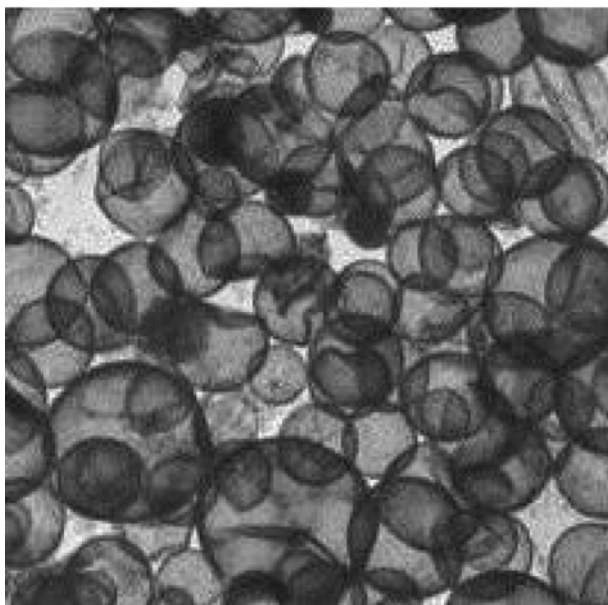


Fig. 3. TEM image of 30 wt% Ni/TiO₂ hollow spheres.

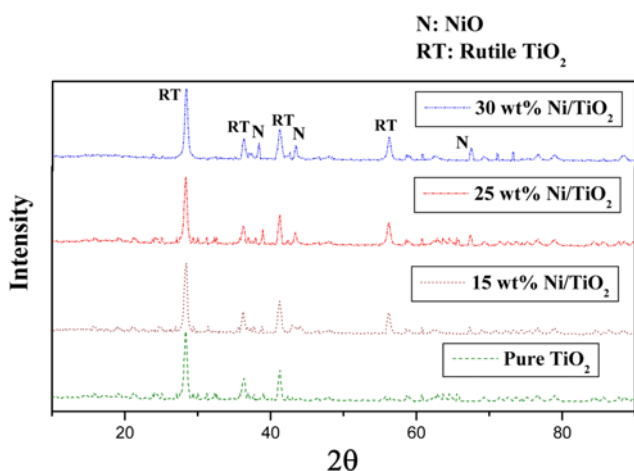


Fig. 4. XRD patterns of 0, 15, 20, 30 wt% Ni-doped TiO₂ hollow spheres.

results have shown that the average particle size of hollow spherical material is 0.8-0.9 μm . The nickel particle loaded over hollow spheres has a size of 10-55 nm.

XRD patterns of TiO₂ hollow sphere materials with and without doping of nickel are shown in Fig. 4. The XRD curves have confirmed the critical growth of rutile TiO₂ in all the catalysts. At the same time, NiO phase has simultaneously grown up in nickel loaded

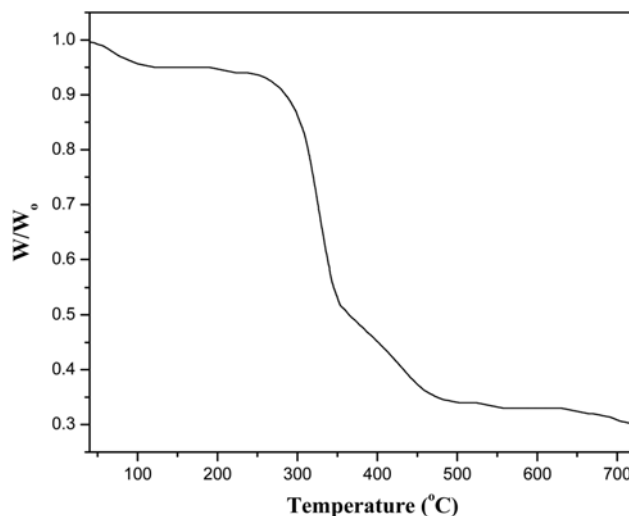


Fig. 5. TG curve of 30 wt% Ni/TiO₂ hollow spheres.

catalysts. Diffraction peaks around 38°, 43°, and 67° are assigned to the formation of (111), (200) and (220) phase of NiO in the materials, respectively; which get more intense with increase in the nickel loading. On the other hand, peaks formed around 28°, 36°, 41°, and 55° have confirmed the presence of (110), (101), (111) and (211) phase, respectively. The peaks ascribed to the NiO phase have not been formed in the pure TiO₂ hollow sphere, whereas rutile titania peaks are most intense in this sample. The only presence of rutile phase, without showing any peaks for anatase form, has confirmed the stability of these catalysts during water electrolysis; as we already know, rutile phase is stable in strong acidic or basic solution. It is clear from the results that both rutile TiO₂ and NiO phase would be responsible in electrocatalytic activity of the hollow sphere materials.

The BET surface area values and pore size distribution values are presented in Table 1. BET surface area values have been evaluated as 63.23, 112.3, 158.9, 173.4 m²/g for 0, 15, 25 and 30 wt% Ni/TiO₂ samples, respectively. It is clear from the results that nickel loading over the hollow spherical structure has influenced considerably the surface area values. It can be assumed that nickel particles during loading have created cracks on the surface, which has resulted in the higher surface area with greater loading of nickel. The pore size values have revealed all the samples as mesoporous materials, which have maintained inclining order with rise in the nickel loading. The catalyst without loading of nickel possesses only 8.27 nm pore size, which has reached the highest value of 18.9 nm for 30 wt% Ni/TiO₂. Therefore, the pore size values have also confirmed the formation of cracks on the surface, which is responsible for greater pore size on the surface.

Table 1. BET Surface area and pore size results of Ni/TiO₂ hollow spheres

Sample	BET surface area (m ² /g)	Langmuir surface area (m ² /g)	Average pore diameter (4V/A) (Å)	BJH adsorption average pore diameter (4V/A) (Å)
Pure TiO ₂	63.23	95.4	85.4	82.7
15 wt% Ni/TiO ₂	112.3	149.34	118.3	114.28
25 wt% Ni/TiO ₂	158.9	215.12	181.25	179.2
30 wt% Ni/TiO ₂	173.4	234.1	192.34	189.77

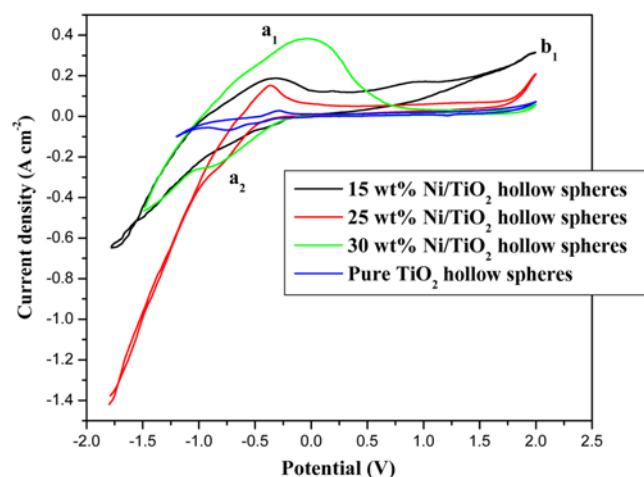


Fig. 6. Cyclic voltammograms of pure TiO_2 and Ni-doped TiO_2 hollow sphere electrocatalysts in PEM water electrolysis cell.

Fig. 5 represents the thermogravimetric curve of uncalcined 30 wt% Ni/ TiO_2 sample. In the TG curve, rapid thermal degradation has started around 280 °C, which ended up at 500 °C; although the trend of degradation changed around 350 °C. The overall degradation phenomena can be assigned to various mechanisms. The rapid degradation resulted in the burning out of organic residues such as PSA latex and surfactant (CTACl) used in the synthesis process.

The cyclic voltammograms of pure TiO_2 and Ni/ TiO_2 hollow sphere electrocatalysts in the PEM water electrolyzer were performed with the scan rate of 100 mV s^{-1} , and the results are compared to the CVs performed in acidic media [14]. Fig. 6 represents the cyclic voltammetric performance of hollow sphere electrocatalysts in PEM water electrolyzer. It is clear that these materials have shown great performance in hydrogen and oxygen evolution reaction in comparison to their electrocatalytic activity in acidic media, although the peak positions are same in both anodic and cathodic region. The peak a_1 , which is actually assigned to the hydrogen desorption phenomenon, is most intense for 30 wt% Ni/ TiO_2 hollow sphere sample, with peak current density value of 0.36 A cm^{-2} , which get reduced in 25, 15 and 0 wt% Ni-doped electrocatalysts to 0.19 A cm^{-2} , 0.15 A cm^{-2} and 30 mA cm^{-2} , respectively; although the results are remarkably improved in comparison to their performances in acidic media [14]. On the other hand, the anodic peak current density at b_1 for oxygen evolution reaction was evaluated as 0.3 A cm^{-2} for 15 wt% Ni/ TiO_2 hollow sphere electrocatalyst. The electrocatalytic activity of 25 and 30 wt% Ni-doped hollow sphere samples in oxygen evolution reaction is comparatively lower in PEM water electrolyzer, but still the anodic peak current density value has been enhanced in great extent to their activity in acidic media. The cyclic voltammograms of pure TiO_2 hollow spheres has confirmed that electrocatalytic performance of the materials is considerably influenced by the nickel loading over them. The peak positions have not changed much with the nickel loading, but the cathodic and anodic peak current density values have diminished remarkably. It is clear from the CV results that their trend in electrocatalytic activity follows the same order both in PEM water electrolyzer and acidic media; only the anodic and cathodic peak current density increased remarkably in the former case. The results have confirmed that the electrocatalysts with more

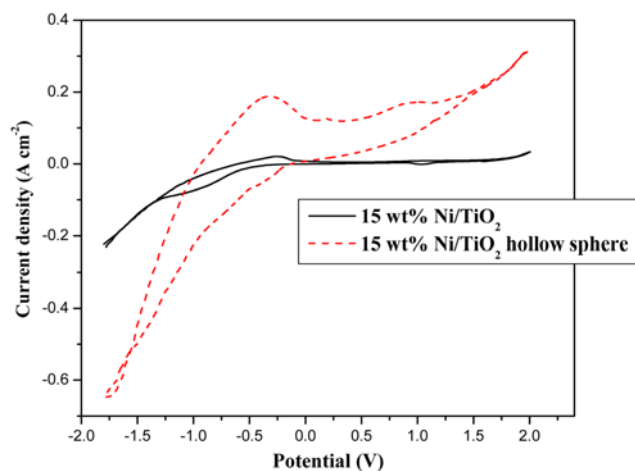


Fig. 7. Comparative cyclic voltammetric results of 15 wt% Ni-loaded TiO_2 non-spherical and hollow spherical materials.

nickel loading over hollow spherical structure are good in hydrogen desorption reaction. On the contrary, the materials with more intense rutile TiO_2 phase (lesser loading of nickel) worked as promising electrocatalysts in oxygen evolution reaction. It is already well explained in our previous work that oxygen deficiency of TiO_2 resulted in the oxygen vacancies on the catalyst surface [14]. Although, pure TiO_2 hollow sphere materials have not worked well as electrocatalyst, due to their poor surface area and small pore diameter values. The basic principle behind better electrocatalytic activity of hollow sphere structure is their large surface area with plenty space for hydrogen and oxygen gases to get absorbed. Nickel loading over hollow spherical structures has greatly induced the surface of the materials, which is seen in SEM images. It was also mentioned that NaCl like cubic structure of NiO phase always exhibits excess of oxygen, which is not kept inside the NaCl structure; this phenomenon creates Ni^{2+} vacancy, promotes the hydrogen desorption process during anodic reaction [19–21]. Moreover, the porous structure of hollow spherical materials influenced the adsorption of oxygen and hydrogen gases all over the spheres.

Fig. 7 presents the comparative cyclic voltammogram results of 15 wt% Ni-doped TiO_2 hollow spherical and non-spherical materials. Clearly, the cathodic and anodic peak current density values are quite lower than those of hollow spherical materials. Thus, it can be concluded that spherical structure with void space has greatly influenced the electrocatalytic activity of the materials.

The outer anodic charge of all the electrocatalysts was calculated from cyclic voltammetric data of water electrolysis in PEM water electrolyzer and aqueous system, and comparative results are shown in Fig. 8. The outer charge (Q_{outer}) represents the available active area during oxygen evolution reaction [22]. The results show huge differences between PEM and aqueous environment as a function of nickel content in electrocatalysts. At lower Ni content, Q_{outer} values are almost similar for PEM and aqueous water electrolyzer. But with increase in the amount of nickel in electrocatalysts, Q_{outer} values get higher to a considerable amount. In the aqueous cell, the electrocatalyst layer requires lateral conductivity, as the electrical support was solid. But in the PEM water electrolyzer, the porous titanium backings have porosities of 50%; thus a loss of 50% surface area

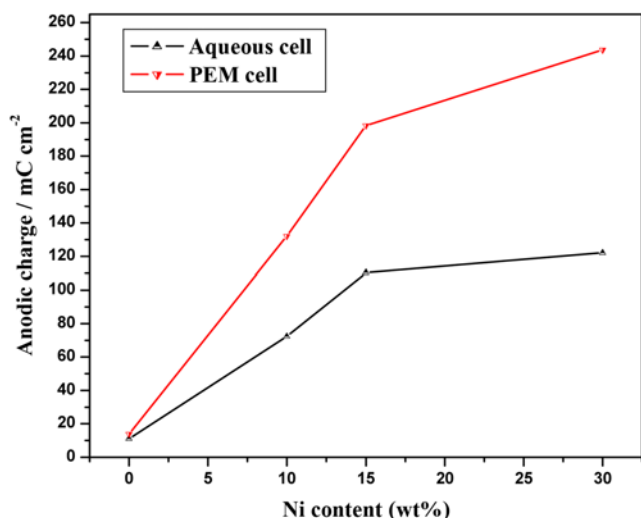


Fig. 8. Outer anodic charge of Ni/TiO₂ hollow sphere electrocatalysts in PEM and aqueous water electrolysis cell.

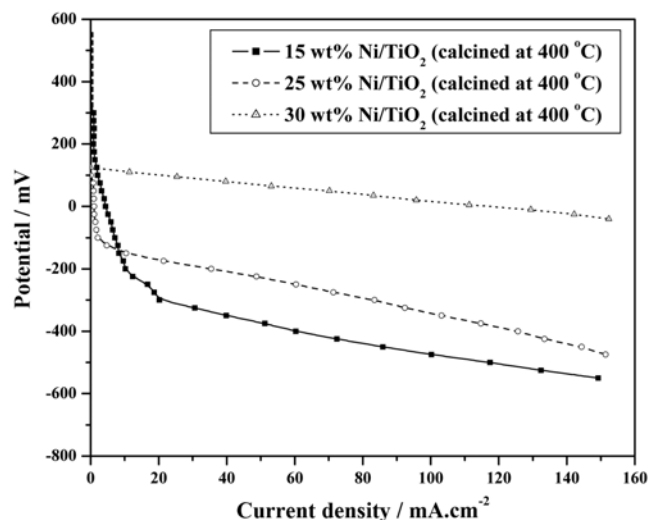


Fig. 9. Galvanostatic polarization curves of Ni/TiO₂ hollow sphere electrocatalysts for HER at 25 °C in PEM water electrolysis cell.

may be reasonable, if the lateral conductivity is very low.

Polarization curves for hydrogen evolution reaction (HER) presented in Fig. 9 were obtained by potentiodynamic method with scan rate of 0.5 mV s⁻¹ at room temperature. It is evident from the results that 30 wt% Ni-doped TiO₂ hollow sphere electrocatalyst has acquired superior catalytic activity in HER compared with others. The catalytic activity for HER followed the declining order as the Ni content in the samples decreases, which supports the cyclic voltammetric results also. The performance of the prepared Ni/TiO₂ hollow sphere electrocatalysts for oxygen evolution reaction (OER) was also evaluated using potentiodynamic method (scan rate: 0.5 mV s⁻¹) at room temperature, which is shown in Fig. 10. The results have shown that at lower current density range 15 wt% Ni-loaded titania electrocatalyst achieved the highest current density at comparatively lower over-potential value, which decreased with rising of nickel content in hollow sphere electrocatalysts. Although the over poten-

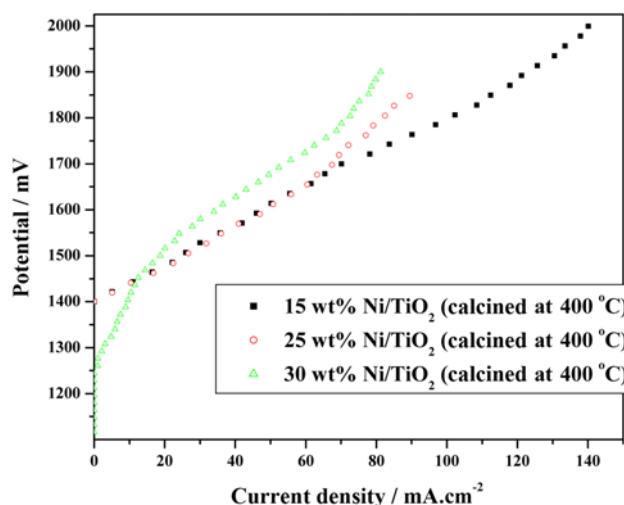


Fig. 10. Galvanostatic polarization curves of Ni/TiO₂ hollow sphere electrocatalysts for OER at 25 °C in PEM water electrolysis cell.

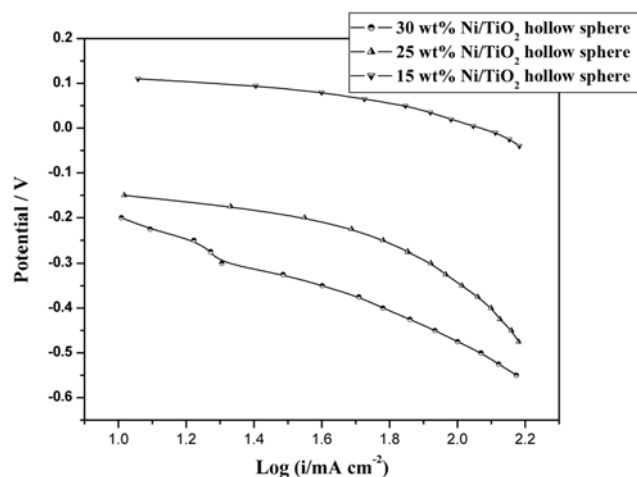


Fig. 11. Tafel plots of Ni/TiO₂ hollow sphere electrocatalysts for HER at 25 °C in PEM water electrolysis cell.

tial values are almost same for 15 and 25 wt% Ni/TiO₂ samples at lower current density range. It is well known that, over potential values are mostly influenced by bubble formation and ohmic resistivity at higher current density range, so it always implies the real electrocatalytic activity of the samples. Thus, we can conclude that 15 wt% Ni/TiO₂ hollow sphere electrocatalyst with more intense rutile TiO₂ phase, is most active in OER process. The oxygen deficient characteristic of this phase influences the greater activity of this sample towards oxygen production. The performance of 15 wt% Ni/TiO₂ hollow sphere electrocatalyst was evaluated up to 140 mA cm⁻²; all other electrocatalysts also produced 100 mA cm⁻² of current density during anodic polarization analysis. From the polarization curves of HER and OER we can conclude that the performance of all the electrocatalysts has been enhanced in PEM water electrolyzer with comparing their electrocatalytic activity in acidic media already mentioned in our previous work [14]. Figs. 11 and 12 show the Tafel plots of all the electrocatalysts in hydrogen and oxygen evolution reactions, respectively. Average Tafel slope values for both

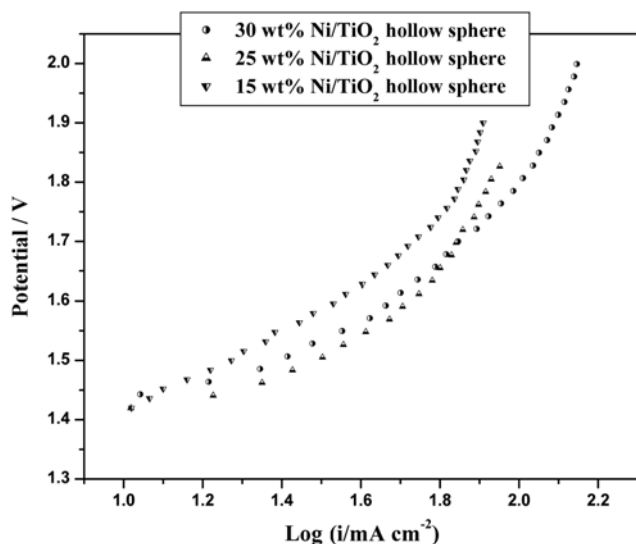


Fig. 12. Tafel plots of Ni/TiO₂ hollow sphere electrocatalysts for OER at 25 °C in PEM water electrolysis cell.

the reactions have also been evaluated using the Tafel equation. Those have been revealed as 70 and 120 mV, respectively, for HER and OER.

The potential at lower current density (1 mA cm⁻²) is usually free of the influence of bubble formation and ohmic resistance. But it is greatly influenced by the formation of bubbles on the surface and also from the ohmic resistance created at higher current density value, which exhibits the real operating conditions. We have presented the comparative cell potential value at lower (1 mA cm⁻²) and higher current density (50 mA cm⁻²) range in Fig. 13 for all the Ni-loaded titania hollow sphere electrocatalysts applied in PEM water electrolyzer and in acidic media. It is clear from the comparative results that the potential values are quite lower in PEM water electrolyzer

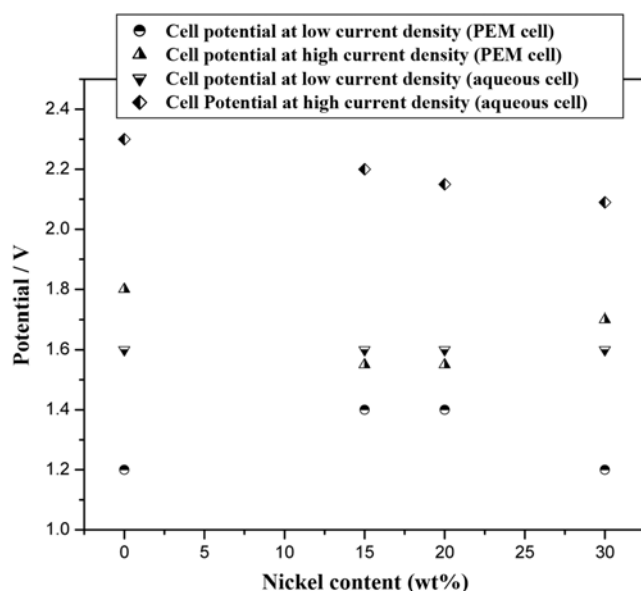


Fig. 13. Cell potential of PEM and aqueous water electrolysis cell at $E_{1\text{mAcm}^{-2}}$ and $E_{50\text{mAcm}^{-2}}$ with various composition of nickel in electrocatalysts.

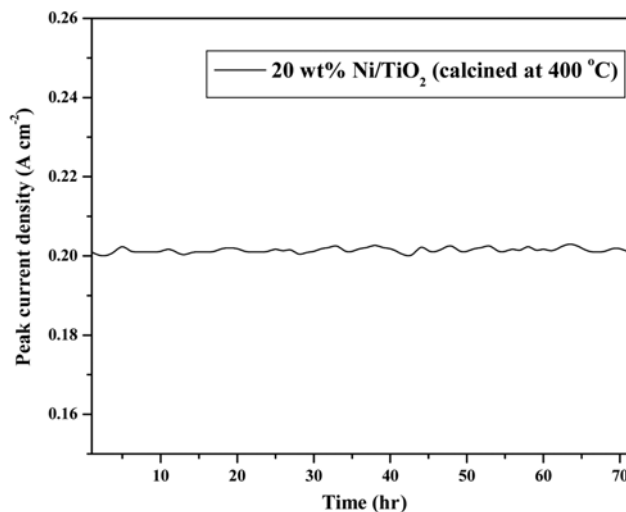


Fig. 14. Potentiodynamic electrocatalytic stability test of 20 wt% Ni/TiO₂ hollow sphere.

irrespective of the current density range. It means the electrocatalytic activity of all the hollow spheres has been enhanced during their application in PEM water electrolysis. It is also clear that the materials with lower nickel content are more active in OER process at comparatively lower over-potential value; which supports the cyclic voltammetric results. Although, pure titania hollow sphere sample exhibited quite higher potential value in higher current density range. In contrast, low current density segments show an inverse trend in over potential value.

From all the electrochemical characterization tests, Ni/TiO₂ hollow sphere materials have been proved as potential electrocatalysts in aqueous cell [14] and in PEM water electrolyzer also. Therefore, we have performed an electrocatalytic stability test with 20 wt% Ni-doped TiO₂ hollow sphere electrocatalyst for 48 h duration in potentiostatic condition in PEM water electrolyzer. In Fig. 14, the anodic peak current density has been plotted against time. It is clear that the anodic peak current density is quite stable after application for long duration also, and this electrocatalyst has maintained an approximate value of 0.20 A cm⁻² as anodic peak current density.

CONCLUSIONS

Nickel-doped titania hollow sphere electrocatalysts with various compositions have been utilized in PEM water electrolyzer. We have synthesized, characterized and examined the electrocatalytic activity of 15, 25 and 30 wt% Ni/TiO₂ hollow spheres in PEM water electrolysis cell, and compared their electrocatalytic performance in aqueous cell, mentioned in our earlier work [14]. XRD patterns have confirmed the formation of rutile TiO₂ and NiO phases in the materials. BET surface area and pore size analysis have shown inclining values with greater loading of nickel, which is highly responsible for their electrocatalytic behavior. SEM images of cyclic voltammograms have confirmed that their trend in electrocatalytic activity follows the same order both in aqueous cell and PEM water electrolyzer; only the anodic and cathodic peak current density increased remarkably in the latter case. 30 wt% Ni-doped titania electrocatalyst has shown the best activity in hydrogen evolution reaction with

0.36 A cm⁻² of peak current density value. On the contrary, 15 wt% Ni/TiO₂ hollow sphere sample is most active in OER with anodic peak current density of 0.3 A cm⁻². Both the values are quite higher than those of their corresponding activities in aqueous cell. The polarization curves have also confirmed that 30 wt% Ni-doped TiO₂ hollow sphere electrocatalyst has acquired superior catalytic activity in HER compared with others. On the other hand, the performance of 15 wt% Ni/TiO₂ hollow sphere electrocatalyst was evaluated up to 140 mA cm⁻² at comparatively lower over-potential value. All the electrocatalysts are electrochemically stable in PEM water electrolyzer during 48 h long potentiodynamic study.

ACKNOWLEDGEMENT

The authors are thankful to DST-SERC, New Delhi for financial assistance during this research work.

REFERENCES

1. M. Peavey, *Fuel from water energy independence with hydrogen*, Merit Products, USA (2003).
2. J. L. Corona-Guinto, L. Carderño-García, D. C. Martínez-Casillas, J. M. Sandoval-Pineda, P. Tamayo-Meza, R. Silva-casarin and R. G. González-Huerta, *Int. J. Hydrog. Energy*, DOI:10.1016/j.ijhydene.2012.12.071 (2012).
3. Y. G. Yoon, G. G. Park, T. H. Yang, J. N. Han, W. Y. Lee and C. S. Kim, *Int. J. Hydrog. Energy*, **28**, 657 (2003).
4. I. Radev, E. Slavcheva and E. Budevski, *Int. J. Hydrogen Energy*, **32**, 872 (2007).
5. H. Beer, *Improvements in or relating to electrodes for electrolytes*, British Patent, 1,147,442 (1969).
6. S. Siracusano, V. Baglio, A. Di Blasi, N. Briguglio, A. Stassi and R. Ornelas, *Int. J. Hydrog. Energy*, **35**, 5558 (2010).
7. Yang Zhang, Lixia Yue, Ke Teng, Shiyong Yuan and M. Hongchao, *J. New Mat. Electrochem. Syst.*, **15**, 271 (2012).
8. S. Trasatti, *Electrochim. Acta*, **29**, 1503 (1984).
9. Y. Z. Zhu, H. B. Chen, Y. P. Wang, Z. H. Li, Y. L. Cao and Y. B. Chi, *Chem. Lett.*, **35**, 756 (2006).
10. M. Fujiwara, M. K. Shiokawa, K. Hayashi, K. Morigaki and Y. Nakahara, *J. Biomed. Mater. Res. A*, **8**, 103 (2007).
11. G. R. Bamwenda, T. Ueisigi, Y. Abe, K. Sayama and H. Arakwa, *Appl. Catal. A*, **205**, 117 (2001).
12. J. Chattopadhyay, H. R. Kim, S. B. Moon and D. Pak, *Int. J. Hydrog. Energy*, **33**, 3270 (2008).
13. J. E. Son, J. Chattopadhyay and D. Pak, *Int. J. Hydrog. Energy*, **35**, 420 (2010).
14. J. Chattopadhyay, R. Srivastava and P. K. Srivastava, *J. Appl. Electrochem.*, **43**, 279 (2013).
15. H. Shiho and N. Kawahashi, *J. Colloid Interface Sci.*, **226**, 91 (2000).
16. N. Kawahashi and H. Shiho, *J. Matter. Chem.*, **10**, 2294 (2000).
17. S. B. Yoon, J. Y. Kim, J. H. Kim, S. G. Park, J. Y. Kim, C. W. Lee and J. S. Yu, *Curr. Appl. Phys.*, **6**, 1059 (2000).
18. E. A. Ticianelli, C. R. Derouin, A. Redondo and S. Srinivasan, *J. Electrochem. Soc.*, **135**, 2209 (1988).
19. G. A. Niklasson and C. G. Granqvist, *J. Mater. Sci.*, **17**, 127 (2007).
20. D. R. Lide, *CRC handbook of chemistry and physics*, 73rd Ed., CRC Press, Boca Raton, USA (2000).
21. P. Lunkenheimer, A. Loidl, C. R. Ottermann and K. Bange, *Phys. Rev. B*, **44**, 5927 (1991).
22. A. Marshall, B. Børrensen, G. Hagen, M. Tsytkin and R. Tunold, *Electrochim. Acta*, **51**, 3161 (2006).